Journal of Mineral Resources Engineering, 7(2): 1-23, (2022)

Imam Khomeini International University
Vol. 7, No. 2, Summer 2022

نشریه مهندسی منابع معدنی
Journal of Mineral Resources Engineering
(JMRE)

Research Paper

Mineral Potential Mapping Using Satellite Images of Sentinel-2, Landsat-8 and ASTER for Iron Ore at Esfordi 1: 100000 Sheet

Ahmadi F.[1], Aghajani H.[2*], Abedi M.[3]

1- Ph.D Student, Faculty of Mining, Petroleum and Geophysics, Shahrood University of Technology, Shahrood, Iran
2- Associate Professor, Faculty of Mining, Petroleum and Geophysics, Shahrood University of Technology, Shahrood, Iran
3- Assistant Professor, School of Mining Engineering, College of Engineering, University of Tehran, Tehran, Iran

Received: 26 Oct. 2020 **Accepted: 06 Mar. 2021**

Abstract: The Esfordi 1:100,000 geological sheet is situated at the Bafgh-Posht-e-Badam district in the central Iran structural zone. Due to the high mineral potentials in this region, many studies have been dedicated to investigate geological phenomena and seek minerals such as iron, phosphorus, lead and zinc. The present study attempts to delimit and explore new mineral potential zones in the Esfordi area through several satellite imagery data. Whereby three types of satellite imagery data including, Sentinel-2, Landsat-8 and ASTER, have been incorporated in this analysis to provide more reliable and powerful outputs. The processing algorithms such as band ratio, false color composites, principal component analysis and directional filtering were used to extract geospatial ore-bearing indicators. Note that areas covered by iron oxides were identified from the band ratios of Sentinel-2 and Landsat-8 images. Based on the color composite images, the rock units that have more impact on mineralization zones were separated. To map alteration zones in association with iron oxides, selective hybrid principal component analysis of bands from ASTER sensor and sentinel-2 satellite data was utilized. By employing directional filtering on the Sentinel-2 images, lineaments were extracted. In addition, prediction-area (P-A) plot was used to determine the weight of each alteration layer and lineament in identifying mineralization zones. The results show that the argillic and propylitic alterations have the lowest association with the mineralization, meanwhile the phyllic alteration with the highest weight has played a significant role in introducing mineralized zones. Outputs show that the mineralization in the study area is mainly related to rhyolite, rhyodacite and carbonate rocks.

Keywords: Mineral potential map, satellite imagery, processing, alteration, prediction-area plot.

How to cite this article
Ahmadi, F., Aghajani, H., and Abedi, M. (2022). *"Mineral potential mapping using satellite images of Sentinel-2, Landsat-8 and ASTER for iron ore at Esfordi 1: 100000 sheet"*. Journal of Mineral Resources Engineering, 7(2): 1-23.
DOI: 10.30479/JMRE.2021.14427.1458

*Corresponding Author Email: *haghajani@shahroodut.ac.ir*

INTRODUCTION

Nowadays, the development of mineral exploration methods has spread across the world. The Bafgh-Posht-e-Badam district in the Yazd Province of Iran is situated at the central Iranian structural zone. This region is well-known as afavourable area in terms of mines and minerals, especially related to iron ores [1-3].

In the central Iranian structural zone, a lot of iron mines exist espicialy in the Bafgh region. As a part of the central Iranian domain, the Esfordi area includes several important iron ore mines, such as Chadormalu, Choghart, Sehchahun and Mishdvan [4,5].

Due to the vastness of the central Iran zone and since this region often has high potential of ore-bearing mineralization, remote sensing studies can be very effective in identifying alteration and new potential zones, which reduce the costs and the time of exploration program significantly [6,7].

The information required to identify different mines can be obtained using different satellite data and processing techniques [8,9].

Yousefi and carranza have developed a prediction-area plot for weighting to indicator/evidence layers [10]. In this method, the logistic function is used to assign fuzzy membership value to continuous spatial evidence values. The logistic function transfers all data to a finite-range of [0-1]. The horizontal axis of the plot contains these values. The two vertical axes in the plot express the percentage of predicted anomalies in the study area and the precentage of the occupied area. The intersection point of this plot will indicate the weight of each layer. This means that the weight of layer will be the most if the intersection point be the highest.

The aim of this study is to identify zones with more favorability for iron ore mineralization in the Esfordi 1: 100,000 geological sheet using remote sensing techniques. Therefore, iron ore potential map is plotted. Areas with the higher potential of iron ore have been identified and introduced in three steps: 1- preparation of evidence layers. 2- computing the weight of each layer and 3- compilation of all evidence layers into a single iron potential map through the geometric mean method.

MATERIALS AND METHODS

In this research, the Band Ratio (BR), False Color Composite (FCC), Principal Component Analysis (PCA) and Spectral Angle Mapper (SAM) methods were used to process multiset satellite imagery data. All evidence layers were weighted using prediction-area plot. Finally, different layers were combined through the geometric mean method and the mineral potential map was prepared.

Two Sentinel-2 image frames (T40SCA and T40RCV numbers on August 20, 2018 and July 31, 2018), one Landsat-8 image frame (161-038 number on July 24, 2019), and three ASTER image frames (two frames on August 10, 2001 and another on July 25, 2001) were downloaded from the U.S. Geological Survey (USGS). Atmospheric corrections were performed before any processing. FLAASH atmospheric correction was used in both Landsat-8 and ASTER data. Sentinel-2 images were corrected using the SNAP software.

FINDINGS AND ARGUMENT

In this study, six evidence layers were prepared which are 1) argillic altertion, 2) propylitic altertion, 3) phyllic alteration, 4) iron oxide alteration, 5) gossan zone and 6) lineaments. After processing satellite data and preparing all evidence layers, the threshold limit for each layer was determined using the value-area fractal method. All evidence layers were reclassified based on the obtained fractal plots. Then, prediction-area plots were prepared for each layer. The normalized density was calculated by dividing the prediction rate by the occupied area. Finally, the weight of each layer was obtained by natural logarithm of this value. The results are summarized in Table 1.

According to Table 1, the argillic and propylitic alteration layers have a weight of zero, so these layers were discarded from the integration process.

The values were transferred to a fuzzy interval (Figure 1A) and the integrated map was divided into six classes using fractal method (Figure 1B). The reclassified map was obtained based on the fractal plot (Figure 1C). Then the prediction-rate plot was prepared (Figure 1D). Based on the intersection point in Figure 1D,

Table 1. Evidence layers extracted from satellite imagery data and assigned weight based on the prediction-area plots

Data	Layer	Method	Prediction Rate	Area	Normalized Density	Weight
ASTER	Argillic	BR, PCA	50	50	1	0
	Propylitic	BR, PCA	50	50	1	0
	Phyllic	BR, PCA	70	30	2.33	0.846
Sentinel-2, Landsat-8	Iron Oxide	BR, PCA	58	42	1.38	0.323
Sentinel-2	Gossan	BR	64	36	1.78	0.575
	Lineaments	Directional Filter	60	40	1.5	0.4

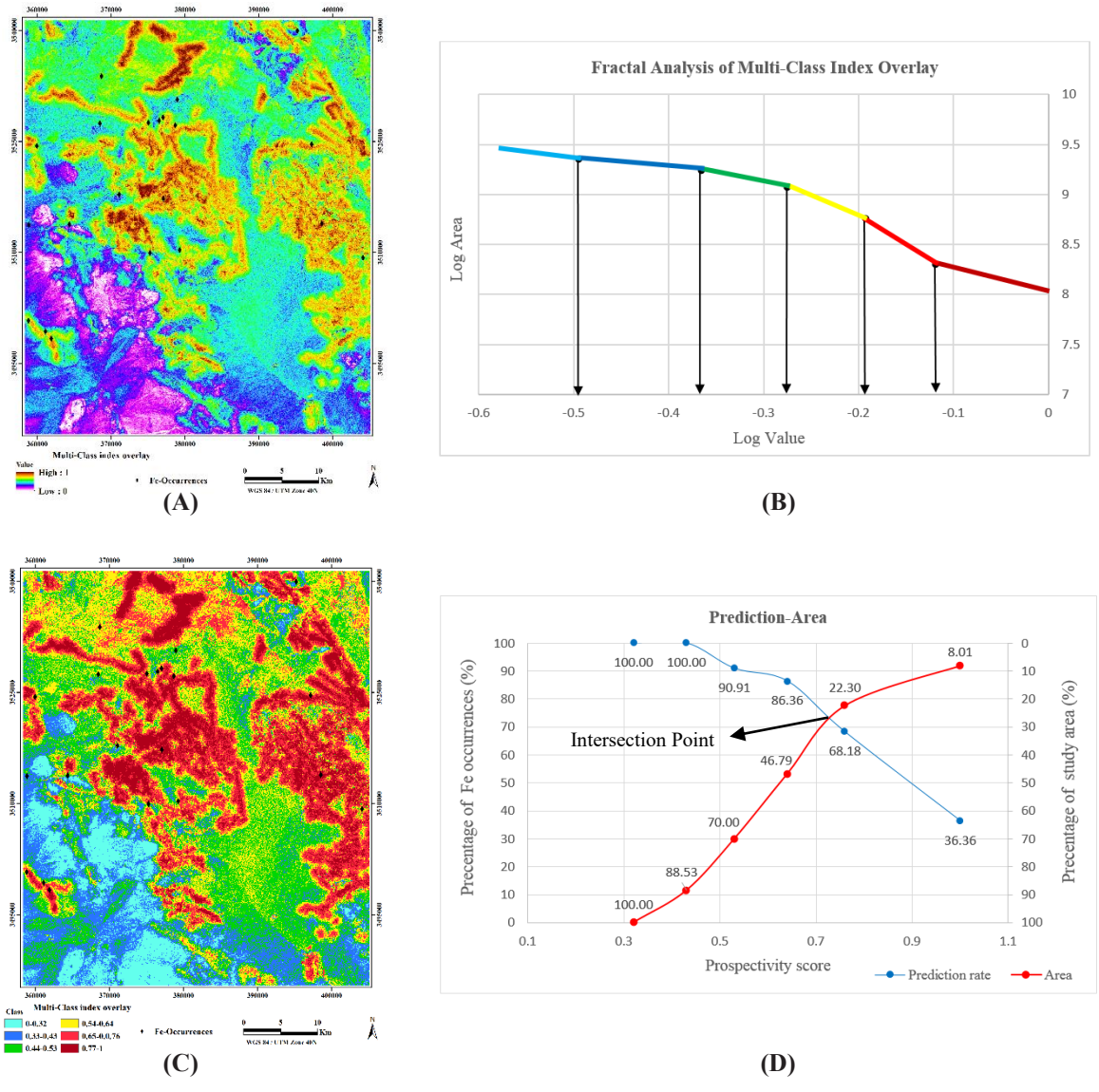

Figure 1. Integrated map of all evidence layers from remote sensing data **A:** fuzzy map, **B:** C-N log-log plot, **C:** reclassified fractal-based evidential map, and **D:** the P-A plot

the integrated map obtained from four evidence layers has occupied 27% of the study area as favorable zones by which 73% of the known Fe occurrences have been delineated. Therefore, the synthesized map has more weight than each single layer as well.

CONCLUSIONS

An integrated map was obtained from all evidence layers through the geometric mean method. According to the intersection point, this layer has occupied 27% of the study area with an ore prediction rate of 73%. According to this map, some regions can be introduced as favorable zone in association with iron mineralization. One of the most important zone among these regions is the SE part of the Esfordi sheet. In addition, in the center and south of the study area -at the edge of carbonate units- are areas with the highest mineral potential. Rhyolite, rhyodacite and calcareous dolomites are the utmost important units associated with the iron-bearing mineralization.

REFERENCES

[1] Förster, H., and Jafarzadeh, A. (1994). "*The Bafq mining district in Central Iran - a highly mineralized Infracambrian volcanic field*". Economic Geology, 89: 1697-1721.

[2] Mohammad Torab, F. (2008). *"Geochemistry and metallogeny of magnetiteapatite deposits of the Bafq Mining District, Central Iran"*. Doctoral Thesis, Faculty of Energy and Economic Sciences Clausthal University of Technology, pp. 131.

[3] Daliran, F., Stosch, H. G., and Williams, P. J. (2009). *"A review of the Early Cambrian magmatic and metasomatic events and their bearing on the genesis of the Fe oxide-REE-apatite deposits (IOA) of the Bafq district, Iran"*. In: Williams, P. (Ed.), Smart Science for Exploration and Mining, 10th SGA Biennial, Townsville, 623-625.

[4] Sadeghi, B., Khalajmasoumi, M., Afzal, P., Moarefvand, P., Yasrebi, A. B., Wetherelt, A., and Ziazarifi, A2013)). *"Using ETM+ and ASTER sensors to identify iron occurrences in the Esfordi 1: 100,000 mapping sheet of Central Iran"*. Journal of African Earth Sciences, 85: 103-114.

[5] Ghorbani, M. (2013*). "Economic geology of Iran"*. Springer, Berlin, pp. 569.

[6] Soe, M., Kyaw, T. A., and Takashima, I. (2005). *"Application of remote sensing techniques on iron oxide detection from ASTER and Landsat images of Tanintharyi coastal area, Myanmar".* Scientfic and Technical Reports of Faculty of Engineering and Resource Science, Akita University, 26: 21-28.

[7] Haihui, H., Yilin, W., Zhuan, Z., Guangli, R., and Min, Y. (2018). *"Extraction of Altered Mineral from Remote Sensing Data in Gold Exploration Based on the Nonlinear Analysis Technology".* In 2018 10th IAPR Workshop on Pattern Recognition in Remote Sensing (PRRS), IEEE, 1-8.

[8] Sabins, F. F. (1999). *"Remote sensing for mineral exploration".* Ore Geology Reviews, 14(3-4): 157-183.

[9] Bishop, C. A., Liu, J. G., and Mason, P. J. (2011). *"Hyperspectral remote sensing for mineral exploration in Pulang, Yunnan Province"*. International Journal of Remote Sensing, 32(9): 2409-2426.

[10] Yousefi, M., and Carranza, E. J. M. (2015). *"Prediction–area (P–A) plot and C–A fractal analysis to classify and evaluate evidential maps for mineral prospectivity modeling".* Computers & Geosciences, 79: 69-81.